THE BEHAVIOUR OF FLOW IN THE IMMEDIATE VICINITY OF A

SLOPING RECTANGULAR CHANNEL WITH FREE OVERFALL

A THESIS SUBMITTED TO

THE GRADUATE SCHOOL OF NATURAL AND APPLIED SCIENCES

OF

MIDDLE EAST TECHNICAL UNIVERSITY

BY

İHSAN KUTLU

IN PARTIAL FULFILLMENT OF THE REQUIREMENTS

FOR

THE DEGREEOF MASTER OF SCIENCE

IN

CIVIL ENGINEERING

NOVEMBER 2005

Approval of the Graduate School of Natural and Applied Sciences

Prof. Dr. Canan Özgen
Director

I certify that this thesis satisfies all the requirements as a thesis for the degree of Master of Science.

Prof. Dr. Erdal Çokça
Head of Department

This is to certify that we have read this thesis and that in our opinion it is fully adequate, in scope and quality, as a thesis for the degree of Master of Science.

Prof. Dr. Metin GER
Co-Supervisor

Assist. Prof. Dr. Şahnaz TİĞREK
Supervisor

Examining Committee Members

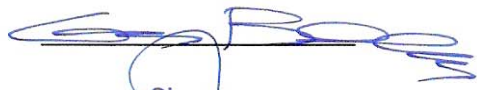Prof. Dr. A.Melih YANMAZ   (METU,CE)

Prof. Dr. Metin GER   (METU,CE)

Assist. Prof. Dr. Şahnaz TİĞREK   (METU,CE)

Assoc. Prof. Dr. Can BALAS   (Gazi U,CE)

Dr. Yurdagül KAYATÜRK   (DSİ)

I hereby declare that all information in this document has been obtained and presented in accordance with academic rules and ethical conduct. I also declare that, as required by these rules and conduct, I have fully cited and referenced all material and results that are not original to this work.

Name, Last Name: İhsan KUTLU

Signature   :

ABSTRACT

THE BEHAVIOUR OF FLOW IN THE IMMEDIATE VICINITY OF A SLOPING RECTANGULAR CHANNEL WITH FREE OVERFALL

KUTLU, İhsan

M.Sc., Department of Civil Engineering

Supervisor: Assist. Prof. Dr. Şahnaz TİĞREK

Co-Supervisor: Prof. Dr. A. Metin GER

November 2005, 38 pages

The flow characteristics of the subcritical and supercritical flows over a free overfall in a rectangular channel are studied experimentally. A series of experiments were conducted in a tilting flume with a wide range of flow rate. Data collected by several researchers are also included. An empirical relationship, which gives the flow rate as a function of the brink depth, the channel bed slope and the bed roughness are confirmed by using data collected in present study. In addition, the behaviors of the ratio of the brink depth to the critical depth according to several flow parameters are examined.

Further, the location of the critical depth in subcritical flows while flow is approaching to the fall is investigated. It is concluded that the location of the critical depth in subcritical flow is a function of the Froude number, channel bed slope and the Manning roughness coefficient. The resemblance or the difference in the occurrence of the profile in sub and supercritical flows examined.

Key Words: Brink Depth, Free Overfall, Discharge Measurement, Critical Depth, Water Surface Profile.

ÖZ

EĞİMLİ DİKDÖRTGEN BİR KANALDAKİ AKIMIN SERBEST DÜŞÜ YAKININDAKİ DAVRANIŞI

KUTLU, İhsan

Yüksek Lisans, İnşaat Mühendisliği Bölümü

Danışman: Yrd. Doç. Dr. Şahnaz TİĞREK

Yardımcı Danışman: Prof. Dr. A. Metin GER

Kasım 2005, 38 sayfa

Nehir rejimi ve sel rejiminin davranış biçimi serbest düşülü dikdörtgen kesitli kanalda deneysel olarak incelenmiştir. Geniş bir veri tabanında değişik eğimlerde deneysel çalışmalar yapılmıştır. Ayrıca başka araştırmacıların çalışmaları da ilave edilmiştir. Bu çalışmada, toplanan veriler kullanılarak, kanaldan geçen debiyi veren, kanal düşü derinliği, eğimi ve pürüzlülüğüne bağlı ampirik bir ilişki verilmiştir. Ayrıca, bazı akım parametrelerine karşı, düşü derinliğinin kritik derinliğe olan oranının davranışı incelenmiştir.

Ayrıca, nehir rejiminde, akım düşüye yaklaşırken kritik derinliğin yeri araştırılmıştır. Nehir rejimindeki kritik derinliğin yerinin Froude sayısına, kanal yatak eğimine ve Manning pürüzlülük katsayısına bağlı olduğu sonucuna varılmıştır. Nehir ve sel rejiminde, profilinin oluşmasında benzerlik yada farklılık incelenmiştir.

Anahtar Kelimeler: Düşü Akım Derinliği, Serbest Düşü, Debi Ölçümü, Kritik Derinlik, Su Yüzü Profili.

ACKNOWLEDGMENTS

To my family…

TABLE OF CONTENTS

LIST OF TABLES

LIST OF FIGURES

xi

Figure

LIST OF SYMBOLS

F_o Froude number

L   length dimension

L_c is critical depth distance from the brink in subcritical flow, whereas it is distance from the brink to where the flow begins to be affected in supercritical flow conditions

Q   discharge

R   hydraulic radius

Re   Reynold's number

S_o bed slope

S_c critical bed slope

b   channel width

g   acceleration due to gravity

n   Manning's roughness coefficient

q   discharge per unit width

x   axis along flow direction

y   axis along gravitational acceleration

y_c critical depth

y_e brink depth

y_o normal depth

y_L is y_c and y_o in subcritical flow and supercritical flow, respectively

ρ density of the fluid

μ viscosity

R^2 correlation coefficient

RMS   root mean square

CHAPTER 1

INTRODUCTION AND REVIEW OF LITERATURE

1.1 Introduction and Literature Review

The overfall occurs when there is a sharp drop at the downstream of an open channel flow. If the flow properties are not affected by the tailwater conditions, it is called as free overfall. This phenomenon can be observed in both natural and artificial channels. It is very common to see this structure in irrigation and drainage channels. When there is a sudden change in bed slope, a drop structure is introduced to the system. They may function as energy dissipaters, too.

Usage of these drop structures as a discharge measuring devices brings two important advantages. First, they are cheap; installation of a gage will be enough. Second, there will not be silting problem, which can be observed in other kind of measuring structures. Therefore, more than seven decades researchers tried to formulate flow rate as a function of the depth over the fall or the brink depth. Due to difficulty of measuring supercritical flow and obtaining slope differing channels, initial studies were concentrated on horizontal bed (Rouse, 1936). Rouse (1936) claimed that the ratio of the brink depth to critical depth on a horizontal channel was 0.715. There are several studies in which the results of Rouse (1936) were examined. Rajaratnam and Muralidhar, (1968) confirmed the result of Rouse (1936). However some other researchers gave higher values; Gupta et al. (1992) reported a value of 0.745, Ferro (1992) reported it to be 0.760 and Bauer and Graf (1971) gave a higher value of 0.781. All the experiments were carried on a confined free overfall. Thus the side walls of the channel are extended beyond the brink. Rajaratnam and Muralidhar (1964a) reported a value of 0.705 for unconfined free overfall.

On the other hand Krajenhoff and Dommerholt (1977); and Bauer and Graf (1971) conducted experiments to observe effect of roughness and slope. However, in subcritical flow the effect of the slope and the roughness could not be observed. This made researchers consider that these two parameters do not affect the flow rate. Moreover, it is widely accepted that the depth of flow at the brink is equal to the critical depth.

Davis et al. (1998) performed an experimental study of the free overfall in a rectangular channel with differing slopes and bed roughness. The relationship between the upstream critical depth and brink depth was explored and found to be influenced by both the slope and the channel bed roughness, with roughness having a greater effect at steeper slopes.

In 2000, a free overfall was constructed in the Hydraulic Laboratory of Middle East Technical University and two experimental studies completed.

Turan (2002) conducted several experiments in a sloping rectangular channel having smooth bed. The equation given by Davis et al. (1998) was reexamined by those additional data. He concluded that further experiments were needed in order to see the effect of bed roughness.

Fırat (2004) examined the characteristics of the supercritical, critical and supercritical flows at the rectangular free overfall in two different bed roughness and different slopes. He proposed an equation two calculate the flow rate if only the brink depth, bed roughness and channel bed slope are known.

Although there are several studies in which the free fall was solved numerically and/or analytically (Southwell and Vaisey, 1946; Strelkoff and Moayeri 1970; Montes 1992; and Özsaraç 2001; Hager, 1983; and Marchi 1993, Ahmad, 2003; Guo, 2005), none of them achieved complete solution because of the unknown pressure

variation over the brink and difficulty involving effect of the roughness in to the problem.

1.2 Scope of the Study

The scope of this thesis is scrutinized flow over a free fall by colleting new data and using previous data. Therefore in the present study flow characteristic near the fall were experimentally observed. The relation between the discharge and the brink depth proposed by Fırat (2004) were confirmed by the data collected in this study. In addition, the flow profiles near the fall in subcritical and supercritical flow were experimentally measured. This topic has been ignored by researchers. Since it is assumed that, the flow at the brink in subcritical flow can be taken equal to the critical depth.

In Chapter 1, brief description of the problem and literature review is given. In Chapter 2, Theoretical Consideration and in Chapter 3 description of experimental set up are given. Chapter 4 is reserved for the results and discussion and in Chapter 5, conclusions are listed.

CHAPTER 2

THEORETICAL CONSIDERATION ON FREE OVERFALL

2.1 General Characteristics of Free Overfall

The overfall refers to the downstream portion of a rectangular channel, horizontal or sloping, terminating abruptly at its lower end. If it is not submerged by the tail water, it is referred to as the free overfall (Rajaratnam et al., 1976).

The free overfall has a distinct importance in hydraulic engineering; it forms the starting point in computations of the surface in a gradually varied flow such as the discharge spills into an open reservoir at the downstream end. Typical free overfall and the parameters are illustrated in Figure 2.1.
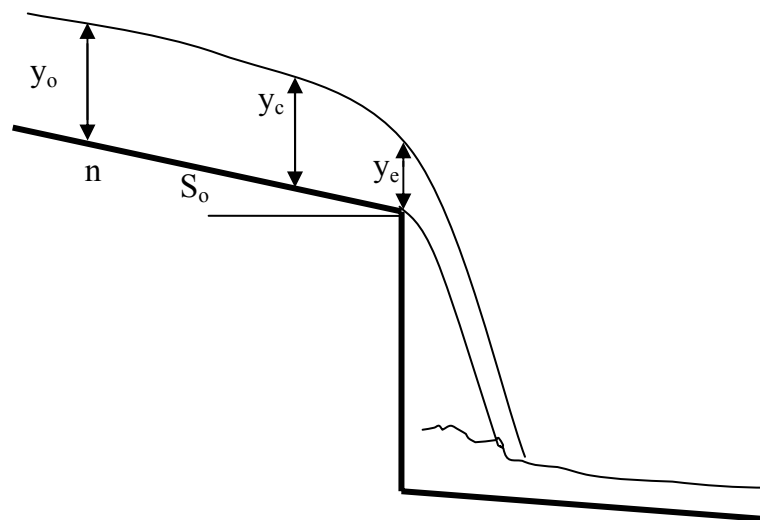
Figure 2.1 The free overfall

In the figure where;

y_o	normal depth	S_o	bed slope
y_c	critical depth	n	Manning's roughness coefficient
y_e	brink depth		

2.2 Dimensional Analysis for the Brink Depth

Based on the following dimensional analysis of the free overflow phenomenon, a series of experiments were scheduled and run. The following variables are involved in affecting the behavior of the flow at a free overfall:

Table 2.1 Parameters involved in dimensional analysis

Parameter	Name	Dimension
y_e	Brink Depth	L
q	Discharge per Unit Width	L^2/T
y_c	Critical Depth	L
y_o	Normal Depth	L
b	Channel Width	L
S_o	Channel Bed Slope	-
g	The Acceleration Due to Gravity	L/T^2
μ	Viscosity of Fluid	M/LT
ρ	Density of Fluid	M/L^3
n or k_s	Manning' s Roughness Coefficient Roughness Height	- L
L_c	Distance From the Brink	L

It must be noted that, based on the discussion of Chow (1959), n is assumed to be dimensionless. Thus, the brink depth y_e is:

$$y_e = f_1(q , y_o, b, \ S_o , g , \ \mu , \ \rho , n) \qquad (2.1)$$

Equation 1 may than be reduced by using Buckingham π theorem with q, y_o, and ρ selected as the repeating variables. Details of the analysis can be found somewhere else (Firat, 2004). Some of terms will not appear in the result; the Reynolds number is neglected on the fact that flow is fully turbulent, the channel is wide thus no width

effect. Later introducing critical depth and discharge relationship in rectangular channel;

$$y_c = \sqrt[3]{\frac{q^2}{g}}$$ (2.2)

or

$$\frac{q}{y_o \sqrt{gy_o}} = (\frac{y_c}{y_o})^{3/2}$$ (2.3)

and replacing y_c/y_o by y_e/y_c and introducing the Manning Equation;

$$V = \frac{q}{y} = \frac{1}{n} R^{2/3} \sqrt{S_o}$$ (in SI system) (2.4)

the following dimensionless parameters can be obtained;

$$\frac{y_e}{y_c} = f_2(F_o, \frac{\sqrt{S_o}}{n})$$ (2.5)

On the other hand, Rajaratnam et al. (1976) proposed the following functional relationship for smooth channels.

$$\frac{y_e}{y_c} = f_3(\frac{S_o}{S_c})$$ (2.6)

Since in the present study the data of Rajaratnam et al. (1976) are included, therefore it is found useful to examine data according to Eq.(2.6), too.

2.3 Dimensional Analysis for the Profile Length

In the present study a new discussion related to the water surface profile near the brink will be introduced. Therefore, a dimensional analysis related to the length of the profile will be introduced. Typical schematic diagram of critical depth distance

6

from the brink $L_{c,sub}$ and corresponding critical depths y_c are given in Figure 2.2 for subcritical flow conditions. In supercritical flow condition, along the profile where the flow begins to be affected from the brink denoted by $L_{c,super}$ and corresponding depths y_o.
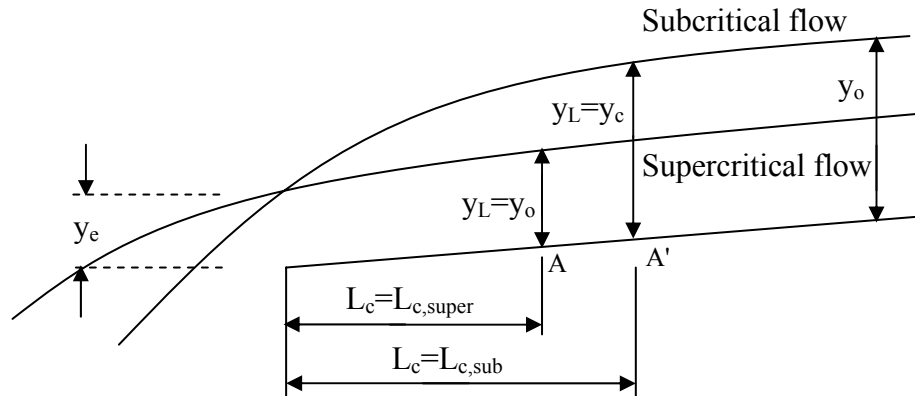
Figure 2.2 Water surface profiles from the brink for both subcritical and supercritical flows

If dimensional analysis is written for L_c;

$$L_c = f_1(q, y_o, b, S_o, g, \mu, \rho, n)$$ (2.7)

Buckingham π theorem is applied again with q, y_o, and ρ selected as the repeating variables;

$$\frac{L_c}{y_L} = f_2(\frac{q\rho}{\mu}, \frac{q}{y_o\sqrt{gy_o}}, \frac{y_o}{b}, n, S_o)$$ (2.8)

Once again, the effect of the Reynolds number and the channel width will be dropped, then;

$$\frac{L_c}{y_L} = f_3(F_o, S_o, n)$$ (2.9)

In addition, all flow conditions are written in one equation to reach the relation of L_c.

$$\frac{L_c}{y_L} = f_4\left(\frac{\sqrt{S_o}/n}{F_o}\right)$$
(2.10)

Thus, with Equation (2.10) $L_{c,sub}$, critical depth distance from the brink in subcritical flow condition and $L_{c,super}$, distance the flow begins to be affected from the brink in supercritical flow condition can be related with flow conditions.

CHAPTER 3

EXPERIMENTAL STUDY

3.1 Description of the Experimental Set-up

The experiments were conducted in a metal rectangular flume 1.00 m in width and 12.06 m in length (Figure 3.1). It had a painted steel bed and the sides of the channel were made of fiberglass. The base of the channel was made of emery paper glued to obtain rough bed. In Figure 3.1 the channel plan and side view are shown. In Figure 3.2 the channel section is shown. Since it is a big channel a steel structure is needed to prevent tilting and deformation at the bottom. The discharge measurements were made by a triangular weir (Figure A.1). Calibration Curve of Triangular Weir is given in Appendix A. The maximum weir capacity is near to 85 lt/s. The sloping bed is regulated by a screw. By the screw the channel can be adjusted to maximum slope of 1/9.22 and to maximum adverse slope of $-1/41.80$.

Water was supplied from a constant head tank through two 20 cm pipes, which were regulated by valves. Water issuing out from the channel was collected in a basin connected to a return channel. An energy dissipater structure is used at the base of the overfall to minimize the fluctuations caused by splashing resulting in a decrease in accuracy of readings in the manometer measuring discharge. In addition, a screen type energy dissipater is used at the entrance of the channel in order to reach uniform flow. A point gauge mounted on rails along the channel to measure water surface and channel bed elevations. Yet, there is another point gauge at the brink section allowed the brink depth, y_e, to be measured. The point gage has an accuracy of ± 0.1 mm (equivalent of 0.1% precision). Measurements were taken for each of the preceding combinations of variables, provided that uniform flow was developed in the flume
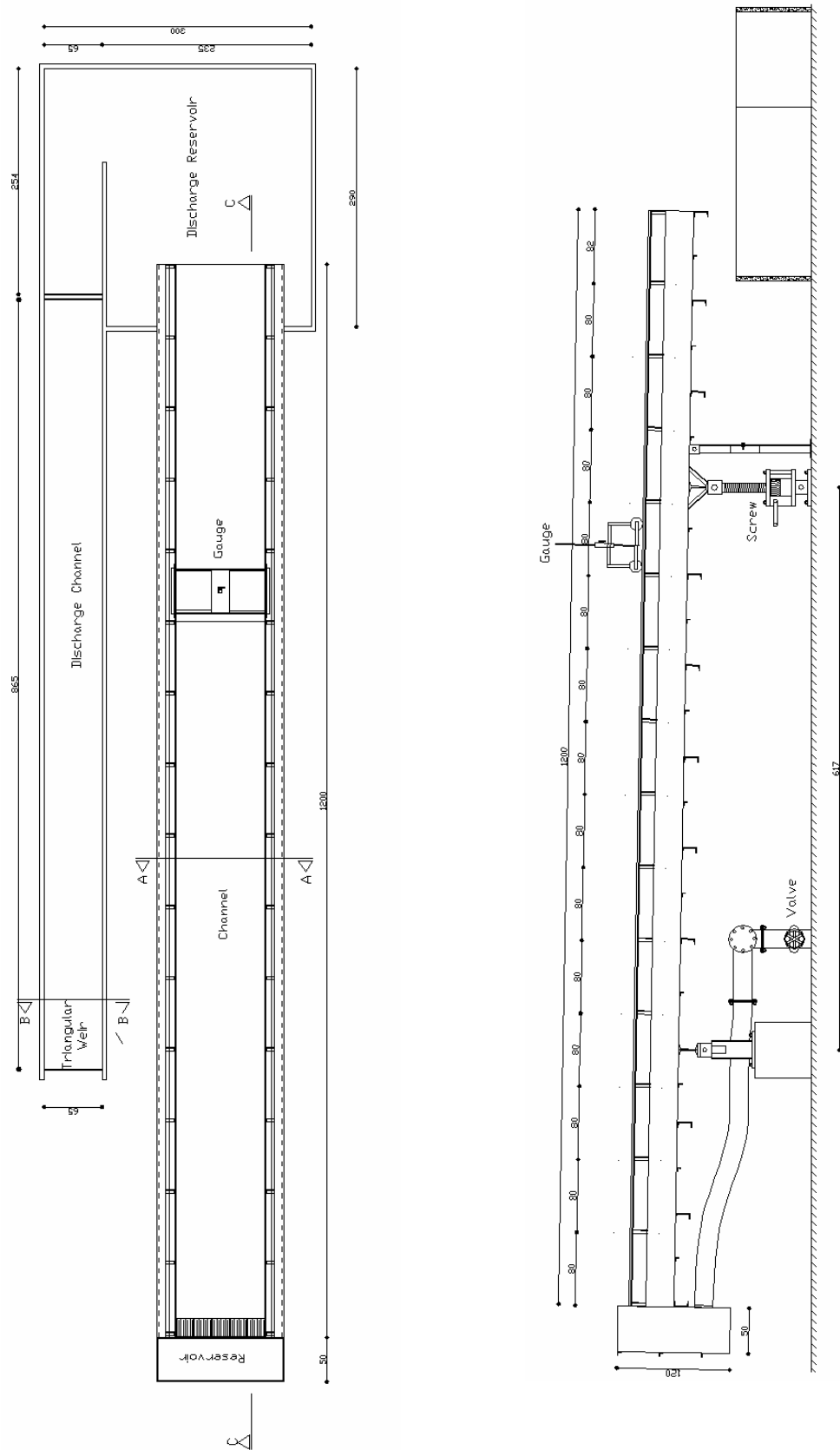
Figure 3.1 The plan view and side view of the experimental set up (After Fırat, 2004)
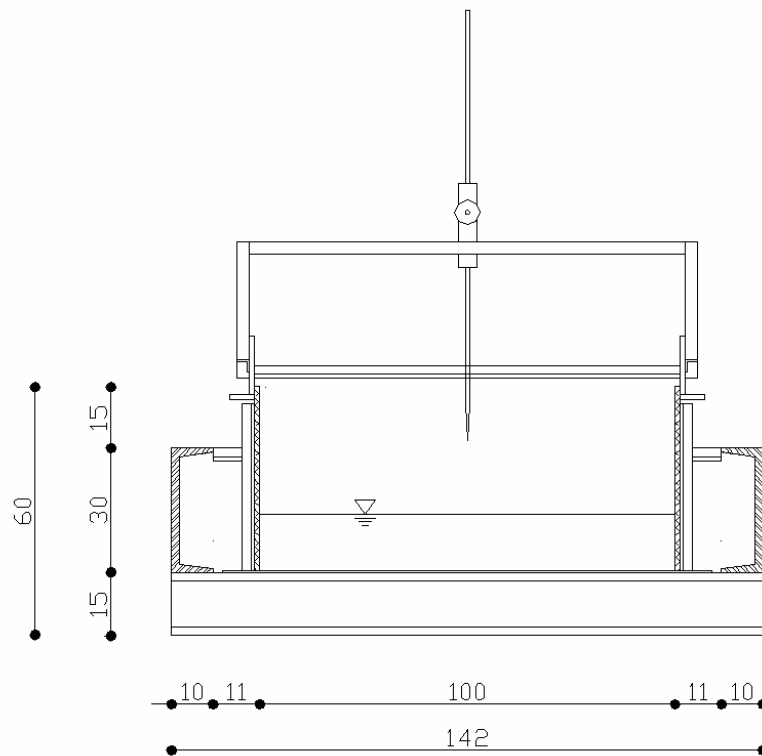
Figure 3.2 The channel section

prior to the overfall. Also Cartens and Carter (1955) as cited in Bauer and Graff (1971), suggested that the channel length should be at least 20 times greater than the critical depth. Two previous studies carried on experiments in the present channel were reported that critical depth is observed to be not deeper than 0.10 m. Thus the suggestion of Cartens and Carter (1955) is satisfied (Fırat, 2004).

3.2 Measurements and Experimental Procedure

In each experiment, discharge, channel bottom elevations, water surface elevations and the brink depths were measured at the mid-point of the channel cross section. The data are given in Appendix-B.

The channel was set to 17 different slopes (8 mild slopes, 5 steep slopes and 4 adverse slopes). The channel slope S_o is regulated by a screw; the channel slope was

11

set to maximum slope of 1/25.84 (0.039) and to maximum adverse slope of $-1/47.85$ (-0.0209). For each experimental set the bottom and the slope of the channel were checked by level.

In each experiment, first the water was pumped to a tank in order to achieve a constant head. The discharge amount was adjusted by the two valves on the supply pipes, which were connected to the constant head tank. By changing the opening of valves at the supply pipe, various values of discharges and hence Froude numbers were obtained. The readings were recorded after a period of time in order for the flow to reach steady flow conditions.

Roughness of the channel n which is equal to 0.0147 is known from earlier study. (Fırat, 2004 see Appendix B). The critical depth of flow, y_c is determined by using discharge,. The normal depth of flow, y_o is calculated from the Manning Equation by iteration and the distance along the profile where the flow begins to be affected from the brink, L_c is computed by plotting of water surface profile for each set of flow.

There are two important details related to experimental studies. First, the brink depth y_e, is usually taken as vertical to the cross-section. However, in some studies it is not well reported. In the present study the brink depth and normal depth, values are taken to be parallel to the gravity direction. Second, the fall in the present study is an unconfined fall. That is the channel wall and bottom of the channel ends at the same location. In previous studies, the researchers were used confined fall following Rouse (1936). These two approaches will be more suitable for field applications.

The measurements were started from 6 m away from the brink section and continued at each 50 cm in 3 m, read at each 30 cm between 3 m and 60 cm from the brink but measurements were taken at each 5 cm between 60 cm and brink section. Locations of readings of water surface profile are depicted in Figure 3.3. In order to measure the brink depths another point gauge which was parallel to the channel bottom was used at the brink section. The measurement of the gauge measuring the normal depths was perpendicular to the channel bottom so a geometrical correction was

12

performed to achieve normal depth values parallel to the gravity direction. From the channel the water discharged to a stilling basin and from this stilling basin it ran out to the return channel. The discharge of the experiment set was measured by the triangular weir on the return channel.
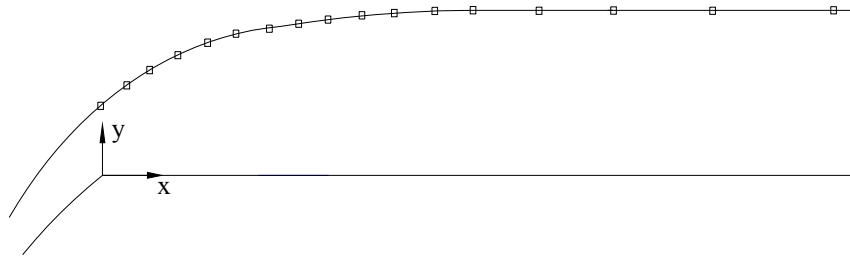
Figure 3.3 Readings of water surface profile

At the end of each experiment set the bed slope; S_o, along the channel water surface profile was read, the brink depth y_e, and the discharge Q values were measured.

CHAPTER 4

DISCUSSION OF RESULTS

4.1 Introduction

In this chapter the data collected in the present study as well as data collected by previous researchers will be reported. Table 4.1 is a summary of the experimental studies examined in the present study.

Table 4.1 Experimental studies examined in the present study

Researchers	Range of Q (lt/s)	Range of S_o	b (m)	n	k_s (mm)	Type of flow	Number of experiments
Present Study	1.75 ~ 61.36	-0.02088 ~ 0.03868	1	0.0147	-	Sub Super	61
Fırat (2004)	1.6 ~ 84.12	0.0003 ~ 0.0394	1	0.0147 ~ 0.009	-	Sub Super	131
Turan (2002)	12.3 ~ 78	0.0017 ~ 0.02	1	0.009	-	Sub Super	26
Davis et al. (1998)	4.3 ~ 45.93	0.0033 ~ 0.02	0.305	0.0147	-	Sub Super	17
Rajaratnam et al. (1976)	28 ~ 229	-0.005 ~ 0.014	0.46		11,9 ~ 18	Sub Super	23

One should note that in the study of Rajaratnam et al. (1976), the value of the Manning roughness coefficient was not reported. Instead the Nikuradse equivalent roughness height were given for three different conditions (k_s=11.9 mm, 13.9 mm

and 18 mm). Therefore, the roughness coefficients are calculated by the Strickler'
equation (Chow, 1959). The roughness coefficients of Rajaratnam et al. data, n is
found very closely to 0.02 for three different roughness heights.

$$n = \phi(\frac{R}{k})k^{1/6} \qquad \text{(k in ft)} \qquad (4.1)$$

Strickler gives an average value of $\phi(R/k)$;

$$\phi(\frac{R}{k}) = 0.0342 \qquad (4.2)$$

Additionally in the present study, brink depth measurements are carried out on four
different adverse slopes. These data are presented in Table B.2.

In the following sections, the relation between the brink depth and the flow
characteristics as well as the geometry will be examined.

4.2 The Relation Between Brink Depth and Critical Depth

The relationship between y_e and y_c for subcritical and supercritical flow are presented
in Figure 4.1a and 4.1b. The best-fit lines shown have been fitted through the data for
each slope tested. The slope of the best-fit lines gives the ratio of y_e/y_c. As it is seen
in Figure 4.1a there is a constant ratio between y_e and y_c for whole slopes in
subcritical flow regime and y_e/y_c ratio is obtained as 0.69. Furthermore, as depicted
in Figure 4.1b, slopes stating supercritical flow condition show a decreasing trend in
y_e/y_c values with increasing slope. For the slopes tested, the coefficients of the best-
fit lines placed through the data are given in Table 4.2, together with R^2 values.

Table 4.2 Best fit y_e/y_c and corresponding R^2 values obtained

Number of Set	Slope	Roughness n	y_e/y_c	R^2	State of Flow
S1	0.00063	0.0147	0.6944	0.9993	Subcritical
S2	0.00166	0.0147	0.6848	0.9981	Subcritical
S3	0.00188	0.0147	0.6568	0.999	Subcritical
S4	0.00194	0.0147	0.7009	1	Subcritical
S5	0.003	0.0147	0.7261	0.9997	Subcritical
S6	0.00388	0.0147	0.6877	0.989	Subcritical
S7	0.00506	0.0147	0.698	0.9975	Subcritical
S8	0.00613	0.0147	0.6922	0.9993	Subcritical
S9	0.00728	0.0147	0.6847	0.9995	Supercritical
S10	0.01325	0.0147	0.6383	1	Supercritical
S11	0.0198	0.0147	0.5706	1	Supercritical
S12	0.0283	0.0147	0.5408	0.9999	Supercritical
S13	0.0388	0.0147	0.4995	0.9985	Supercritical
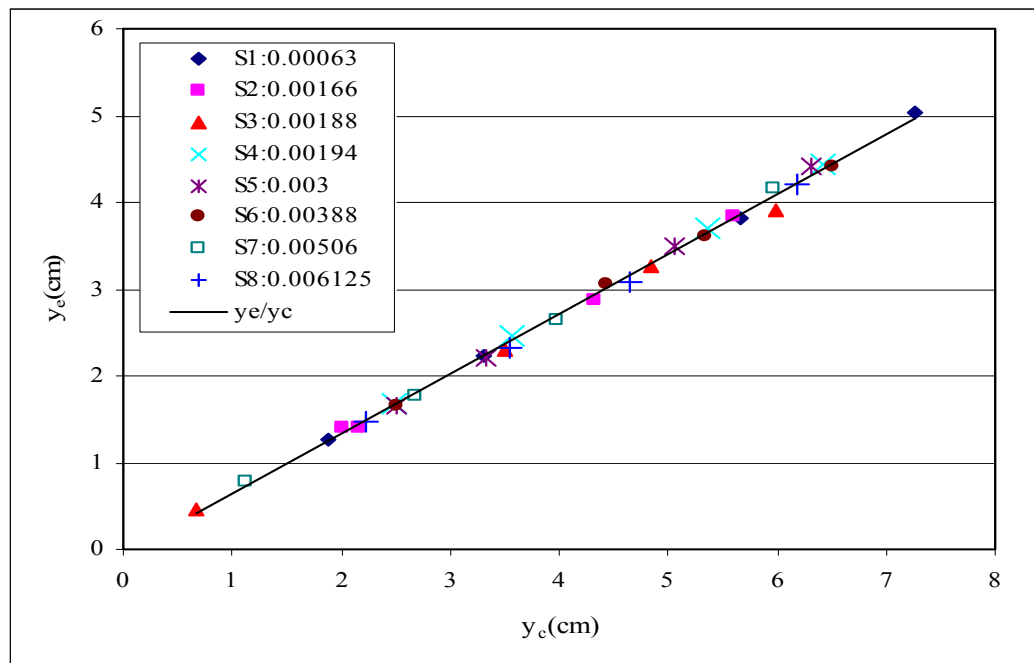
Figure 4.1a Relationship between y_e and y_c with Best-Fit line for all slope in subcritical flow
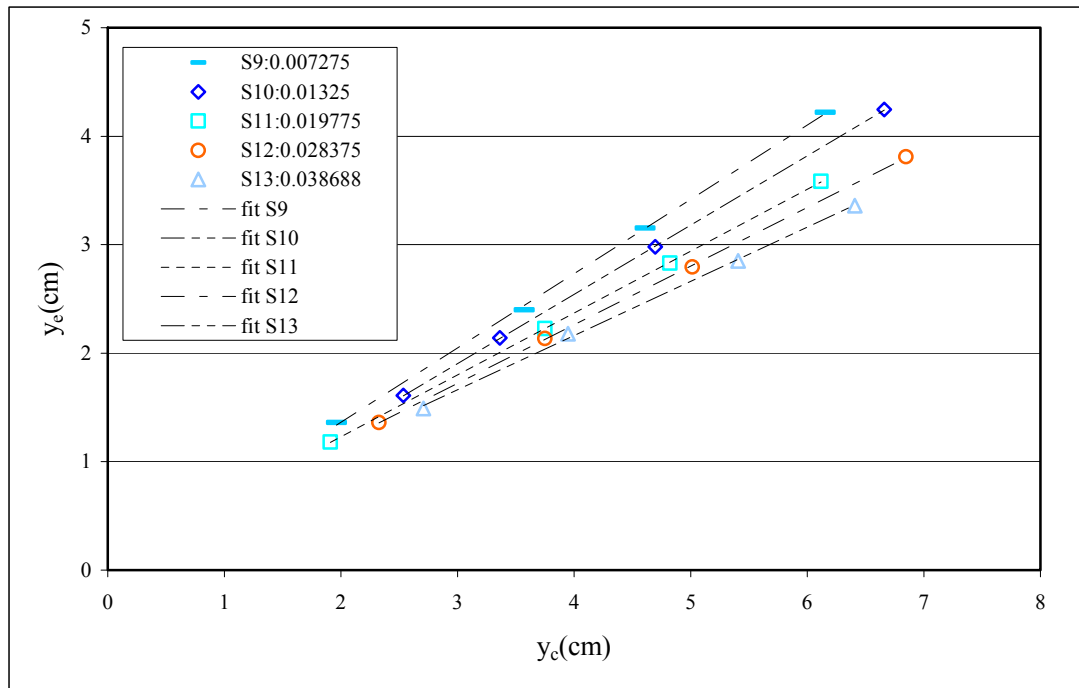
Figure 4.1b Relationship between y_e and y_c with Best-Fit lines for each slope in supercritical flow

4.3 Variation of y_e/y_c with F_o

As y_e/y_c is influenced by S_o and n, a function was sought that encompasses these variables. Upstream Froude Number, F_o, is influenced by S_o and n. Figure 4.2 gives plots y_e/y_c against F_o. In this figure, beside present study, also studies of Davis et al.(1998), Fırat (2004), Rajaratnam et al. (1976) and Turan (2002) are included. The best-fit line shown has been fitted through the data for all researchers. The equation and the R^2 values are given below:

$$\frac{y_e}{y_c} = -0.101(F_o) + 0.74 \qquad\qquad R^2=0.75 \qquad\qquad (4.3)$$
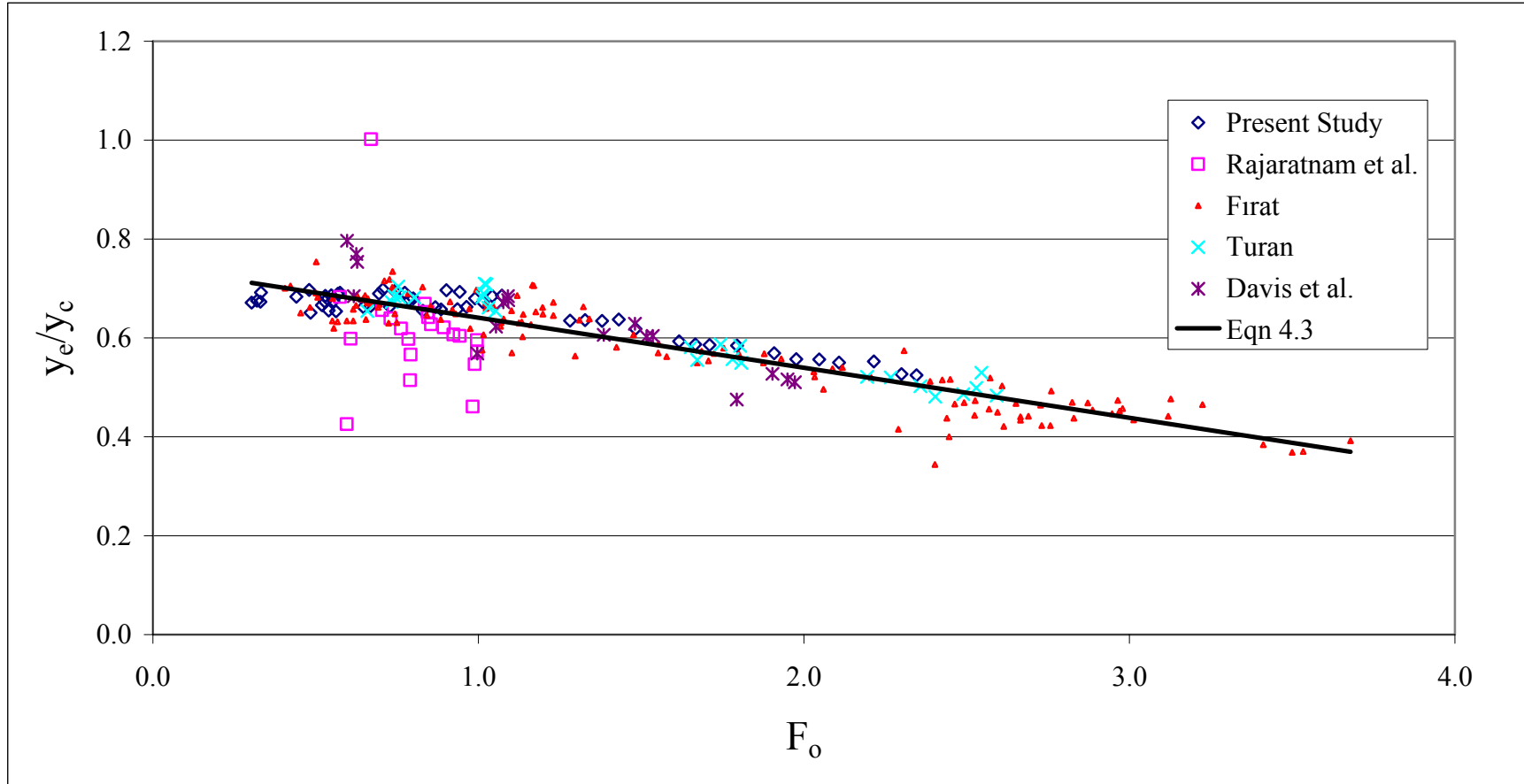
Figure 4.2 Variation of y_e/y_c with F_o for the combined data

4.4 Variation of y_e/y_c with $\dfrac{S_o}{S_c}$

The relationship between y_e/y_c with $\dfrac{S_o}{S_c}$ for five researchers' (Present study (2005), Davis et al.(1998), Fırat (2004), Rajaratnam et al. (1976) and Turan (2002)) studies are presented in Figure 4.3. The best-fit line shown has been fitted through the data for all researchers' slope tested. As it is seen in Figure 4.3, for the slopes, the y_e/y_c values increases, $\dfrac{S_o}{S_c}$ ratio decreases. From the figure it can be deduced that Manning's roughness coefficient n, has no significant effect when comparing Present study to Turan (2002). Also channel width, b, again has no influence on the relationship with comparing Present study to Davis et al.(1998). For all the data tested, the coefficient of the best-fit line is given below together with R^2 values.

$$\frac{y_e}{y_c} = -0.0245(\frac{S_o}{S_c}) + 0.6754 \qquad\qquad R^2=0.77 \qquad\qquad\qquad (4.4)$$
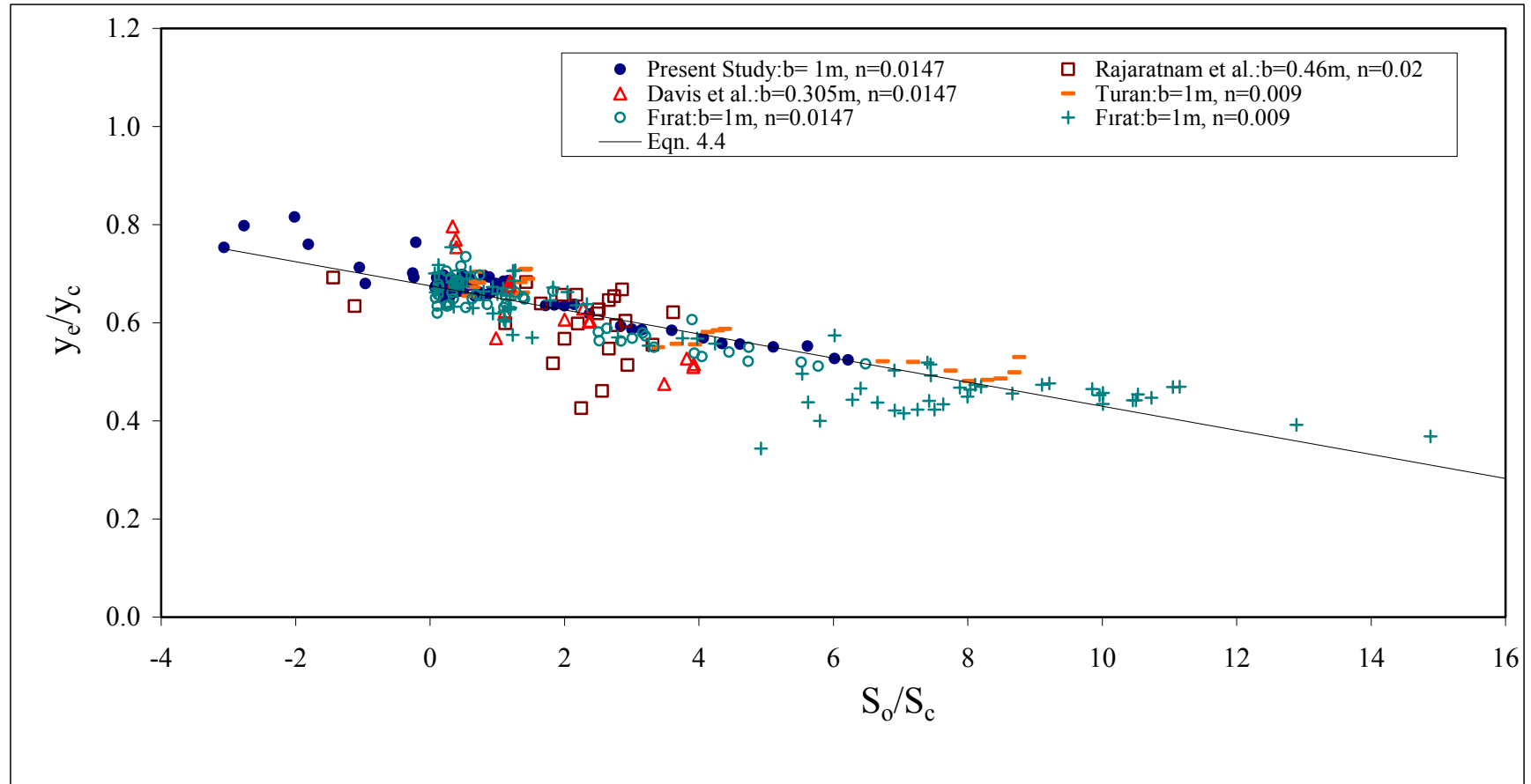
Figure 4.3 Variation of y_e/y_c with S_o/S_c

4.5 Variation of y_e/y_c with y_o/y_c

As a result of dimensional analysis it is shown that y_e/y_c may be related to y_o/y_c. This can be only implicit way to predict discharge with different input data. Since unknown parameter, yc appears on the both axis. This relationship is given in Figure 4.4. The y_e/y_c values with corresponding y_o/y_c values of the present study and other researchers' are given. It can also be deduced from Figure 4.4 the spreading of subcritical values that of y_o/y_c values greater than or equal to 1, is linear which is reported also by Bauer and Graf (1971) and Kraijenhof and Dommerholt (1977), However the distribution of supercritical values that of y_o/y_c values less than 1, is polynomial. Combining the values of all data yields a conditional relationship given below:

$$\frac{y_e}{y_c} = -0.51\left(\frac{y_o}{y_c}\right)^3 + 0.36\left(\frac{y_o}{y_c}\right)^2 + 0.83\left(\frac{y_o}{y_c}\right) \quad \text{RMS=0.035} \quad \frac{y_o}{y_c}<1 \qquad (4.5a)$$

$$\frac{y_e}{y_c} = 0.68 \qquad\qquad\qquad \text{RMS=0.063} \quad \frac{y_o}{y_c}\geq 1 \qquad (4.5b)$$

As it seen from the above equations for the critical flow where $y_o/y_c = 1.00$ the value of y_e/y_c yields to 0.68, and also the peak point of the equation occurs where $y_o/y_c = 1$ representing the critical flow. The subcritical values, that are the values satisfying the condition $y_o/y_c>1.00$, disperse linearly as inferred from Figure 4.4. In summary, Equation 4.5a and 4.5b contain 3 phases of flow as supercritical, critical and subcritical flow.
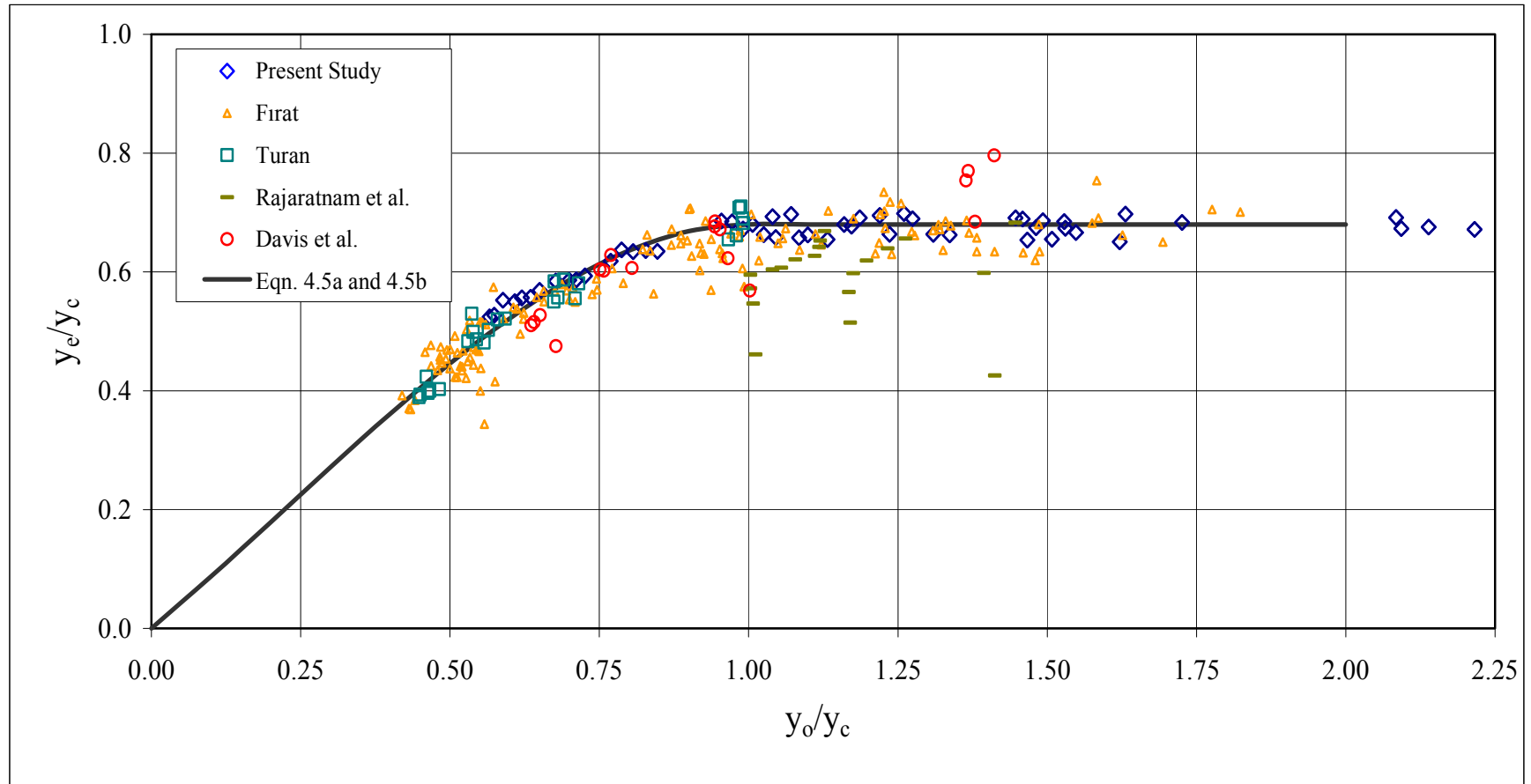
Figure 4.4 Variation of y_e/y_c with y_o/y_c of all researchers' data

4.6 Variation of y_e/y_c with $\dfrac{\sqrt{S_o}}{n}$

The relationship between y_e/y_c with $\sqrt{S_o}/n$, as depicted in Figure 4.5, suggests that $\sqrt{S_o}/n$, as it is a dimensionless parameter in Equation, might be a better variable to explain variation of y_e/y_c. As depicted, in Figure 4.5 the magnitude of y_e/y_c ratio depends on the type of flow regime on roughness and slope. However the effect of slope and roughness combined in a single term, $\sqrt{S_o}/n$, as suggested by Eqn.4.6a and 4.6b which are proposed by Tiğrek et al. (2005), if this term is less than 5 (subcritical flow), y_e/y_c ratio becomes constant. If $\sqrt{S_o}/n$ value is larger than 5 (supercritical flow), y_e/y_c ratio is affected by $\sqrt{S_o}/n$ as given in Equation 4.6b. In this study, data of five researchers (Present study (2005), Davis et al.(1998), Fırat (2004), Rajaratnam et al. (1976) and Turan (2002)) are tested, this equation and RMS values are given below;

$$\frac{y_e}{y_c} = 0.683 \qquad\qquad RMS = 0.032 \qquad\qquad \frac{\sqrt{S_o}}{n} \leq 5 \qquad (4.6a)$$

$$\frac{y_e}{y_c} = 0.773 - 0.018\frac{\sqrt{S_o}}{n} \qquad RMS = 0.027 \qquad\qquad \frac{\sqrt{S_o}}{n} > 5 \qquad (4.6b)$$

For each data point on the figure, y_e/y_c is obtained by finding the best fit of data measured for each slope tested.
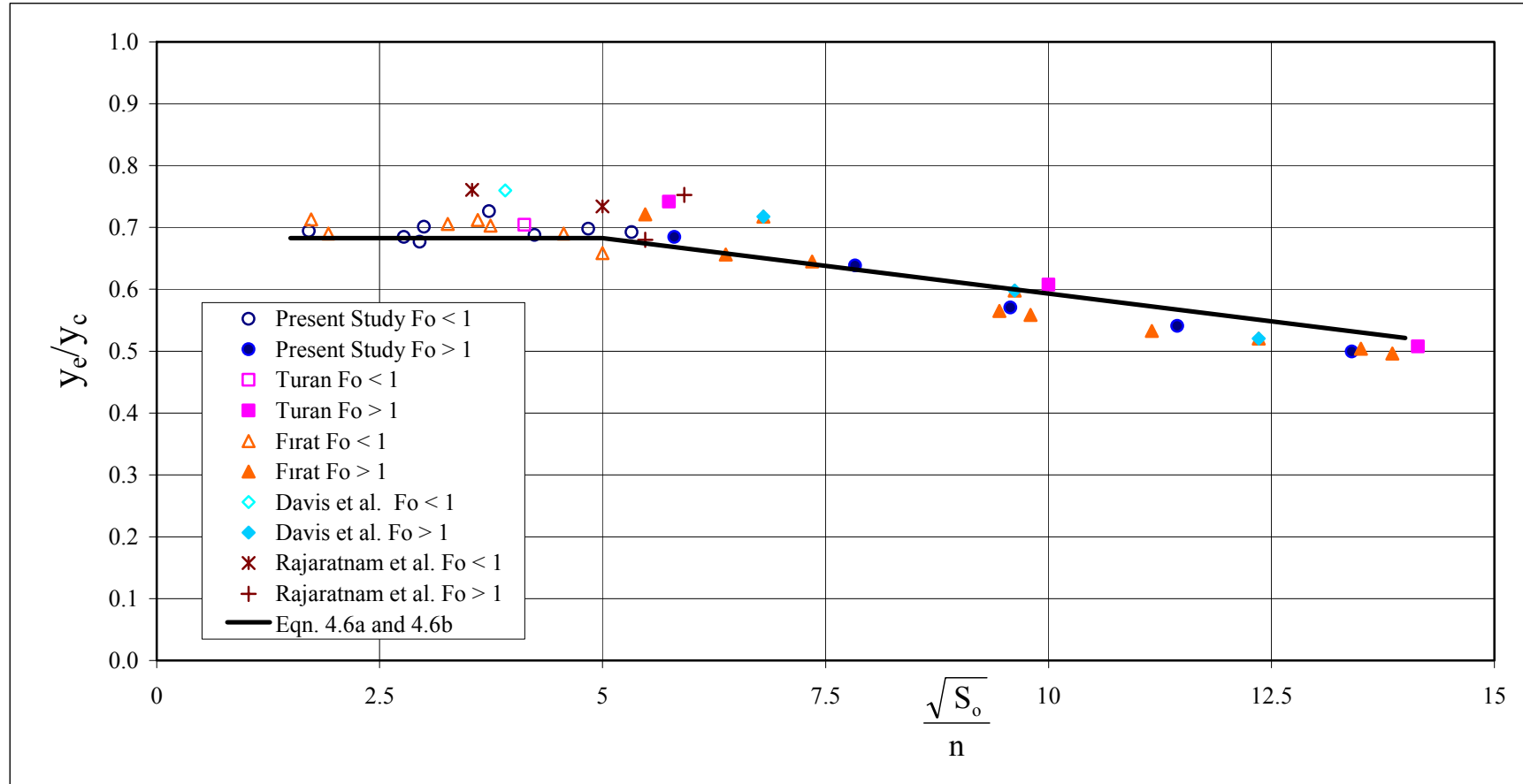
Figure 4.5 Relationship between y_e/y_c with $\sqrt{S_o}/n$

4.7 Discharge Prediction

The flow rate can be predicted by using the appropriate forms of equations presented above for two combinations of known input parameters, namely $y_e/y_c = f\left(\sqrt{S_o}/n\right)$ and $y_e/y_c = f\left(y_o/y_c\right)$. The former relation given in Figure 4.5, that in $y_e/y_c = f\left(\sqrt{S_o}/n\right)$.

Equations 4.6a and 4.6b can be rewritten by replacing y_c by $\sqrt[3]{\dfrac{q^2}{g}}$ as (in SI system):

$$\frac{y_e}{\sqrt[3]{q^2}} = 0.319 \qquad\qquad \text{for} \qquad\qquad \frac{\sqrt{S_o}}{n} \leq 5 \qquad (4.7a)$$

$$\frac{y_e}{\sqrt[3]{q^2}} = 0.361 - 0.0084\frac{\sqrt{S_o}}{n} \qquad\qquad \text{for} \qquad\qquad \frac{\sqrt{S_o}}{n} > 5 \qquad (4.7b)$$

In this form, for known channel characteristics (i.e. S_o and n) for the determination of unit discharge q, the measurement of brink depth is sufficient.

From Equation 4.7a-b a design formula for discharge measurement with known brink depth y_e, Manning's roughness coefficient n, and channel bed slope S_o is obtained. Equation 4.7a-b can be rearranged as (in SI system):

$$q = 5.55 y_e^{3/2} \qquad\qquad \text{for} \qquad\qquad \frac{\sqrt{S_o}}{n} \leq 5 \qquad (4.8a)$$

$$q = \left(\frac{n}{0.361n - 0.0084\sqrt{S_o}}\right)^{3/2} y_e^{3/2} \qquad \text{for} \qquad\qquad \frac{\sqrt{S_o}}{n} > 5 \qquad (4.8b)$$

25

The validity of Equation 4.8a-b is checked by using Present and Rajaratnam (1976) studies as control data. Equation 4.8a-b is used to calculate the discharges based on the y_e, S_o and n values as reported by the authors. The determined values are compared with the respective discharge values reported by them. The best-fit lines are illustrated with $\mp 10\%$ confidence interval to confirm Equation 4.8a-b with the control data collected by other researchers in Figure 4.6a and 4.6b.

As the correlation turns out to be good; it can be deduced that the Equation 4.8a-b derived from the all experimental study, is valid.

Equation 4.8a-b can be used as a very practical discharge computation mean in field studies by hydraulic engineers due to the fact that there is only brink depth to be measured since slope and roughness of the channel are fixed or determined before. This equation can be presented as an alternative and more practical measurement device to the parshall flume, which is designed to exterminate the sediment problem occurring behind the weirs, which are used to measure discharge. In addition, since it is very hard to design and operate the parshall flume, it is very advantageous to use this device in which no other special design is needed. Further if the brink depth is needed for a design of fall Equation 4.8a-b can be used for a given discharge, slope and Manning's roughness coefficient.
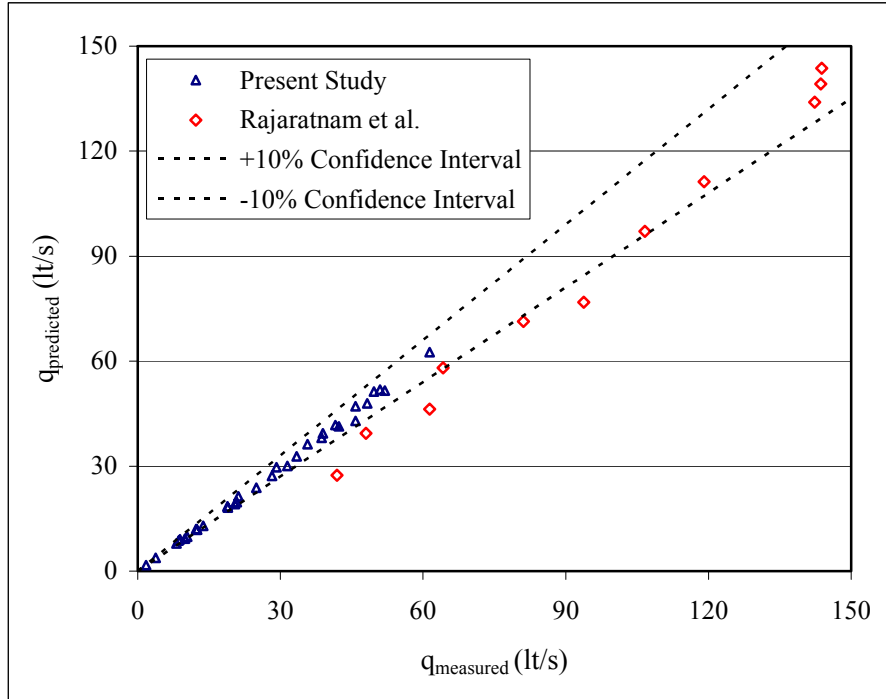
Figure 4.6a Comparison of Equation 4.8a with experimental data of Present study
(2005) and Rajaratnam et al. (1976)
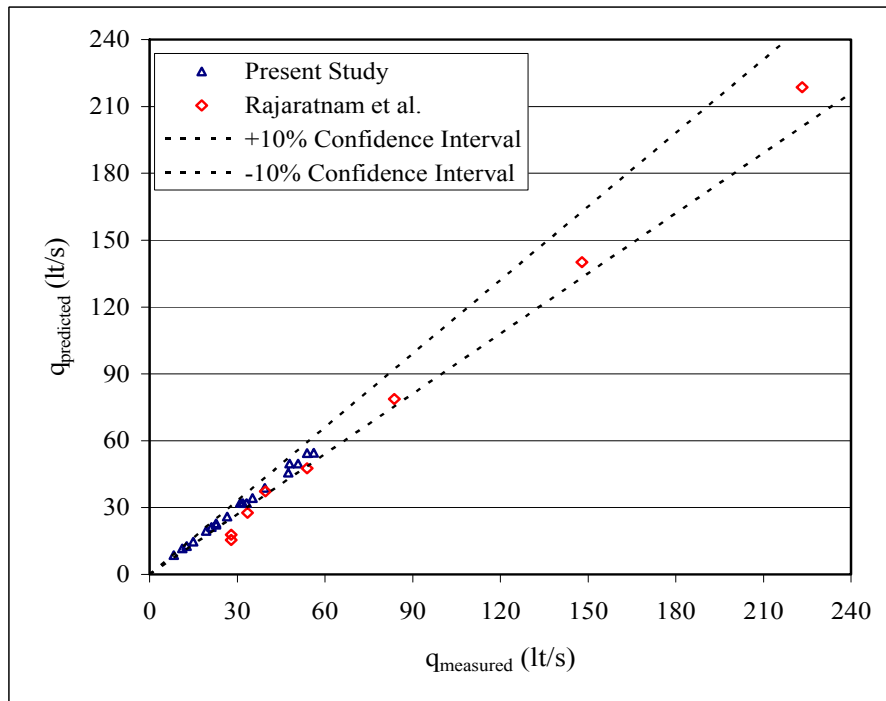
Figure 4.6b Comparison of Equation 4.8b with experimental data of Present study
(2005) and Rajaratnam et al. (1976)

4.8 The Surface Profile in the Vicinity of a Free Overfall

The surface profile in the immediate vicinity of a free overfall is schematically illustrated in Figure 4.7, below.
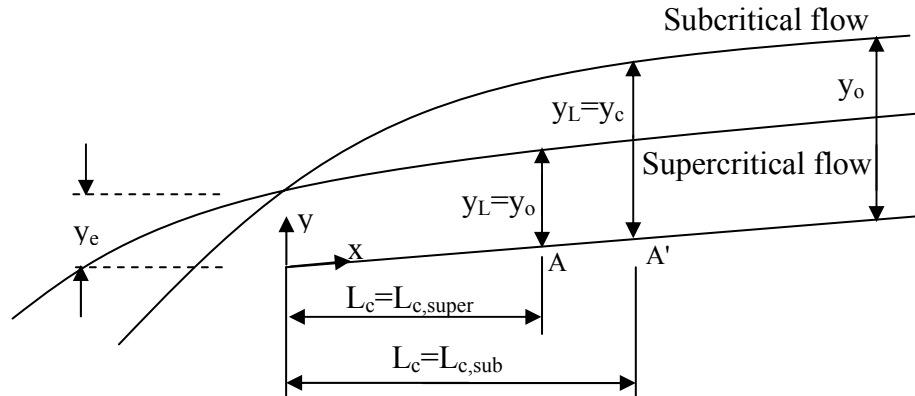
Figure 4.7 Water surface profiles from the brink for both subcritical and supercritical flows

As depicted in the figure, the immediate vicinity is defined as the region between the brink and the point (i.e. A or A') downstream of which variation of flow depth takes places in subcritical and supercritical regime. In other words, with reference to Figure 4.7, the depth at the most downstream of the regime is y_e and the depth upstream the regime, y_L is y_c and y_o for the subcritical and supercritical uniform flows, respectively.

4.9 Variation of L_c/y_L with $\dfrac{\sqrt{S_o}/n}{F_o}$ in Subcritical and Supercritical Flow

There is a linear relationship between L_c/y_L and $\dfrac{\sqrt{S_o}/n}{F_o}$ for the subcritical flow condition as shown in Figure 4.8. Due to the availability of the data in the literature, present study has been compared with Turan's study. An appreciate curve is fitted

28

for these points of two researchers. Equation and the R^2 values are given in Table 4.3.
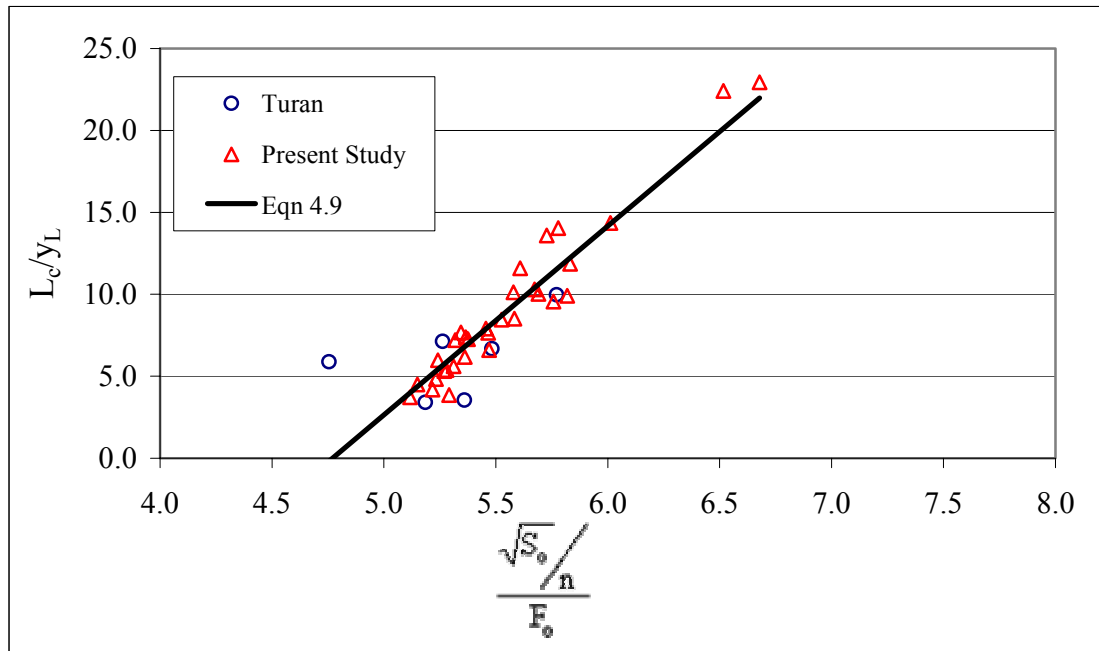
Figure 4.8 Variation of L_c/y_L with $\dfrac{\sqrt{S_o}/n}{F_o}$ in subcritical flow

There is a linear relationship between L_c/y_L and $\dfrac{\sqrt{S_o}/n}{F_o}$ for the supercritical flow condition as shown in Figure 4.9. Due to the availability of the data in the literature, present study has been compared with Turan's study. An appreciate curve is fitted for these points of two researchers. Equation and the R^2 values are given in Table 4.3.
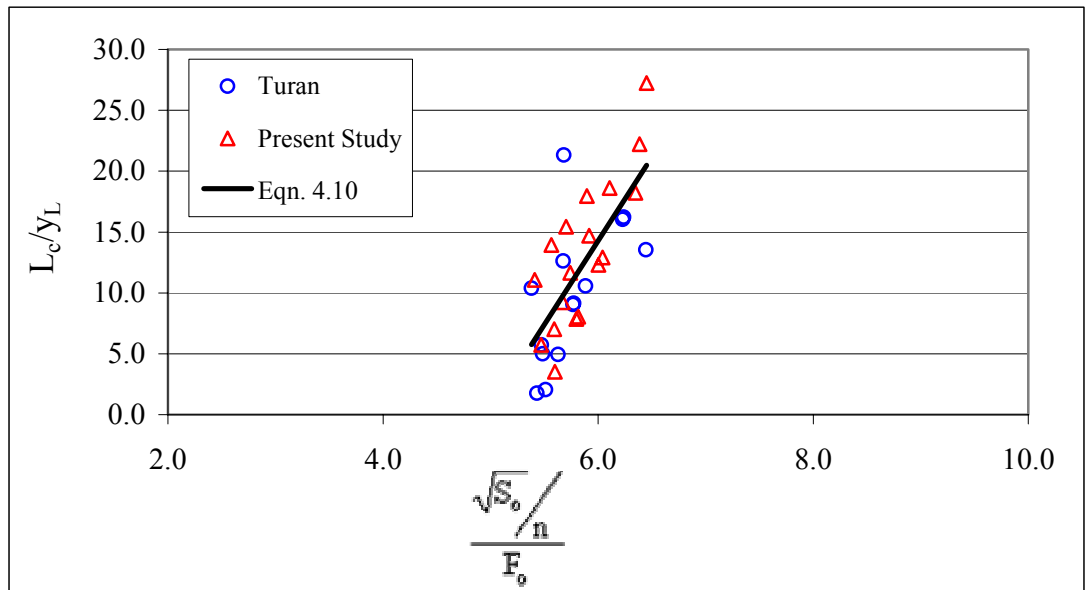
Figure 4.9 Variation of L_c/y_L with $\dfrac{\sqrt{S_o}/n}{F_o}$ in supercritical flow

As depicted in Figure 4.10, when the two relationships for subcritical and supercritical flow conditions combined, it is observed that there is no significant difference between two flow conditions. An appreciate curve is fitted for all data of two researchers. Equation and the R^2 values are given in Table 4.3.
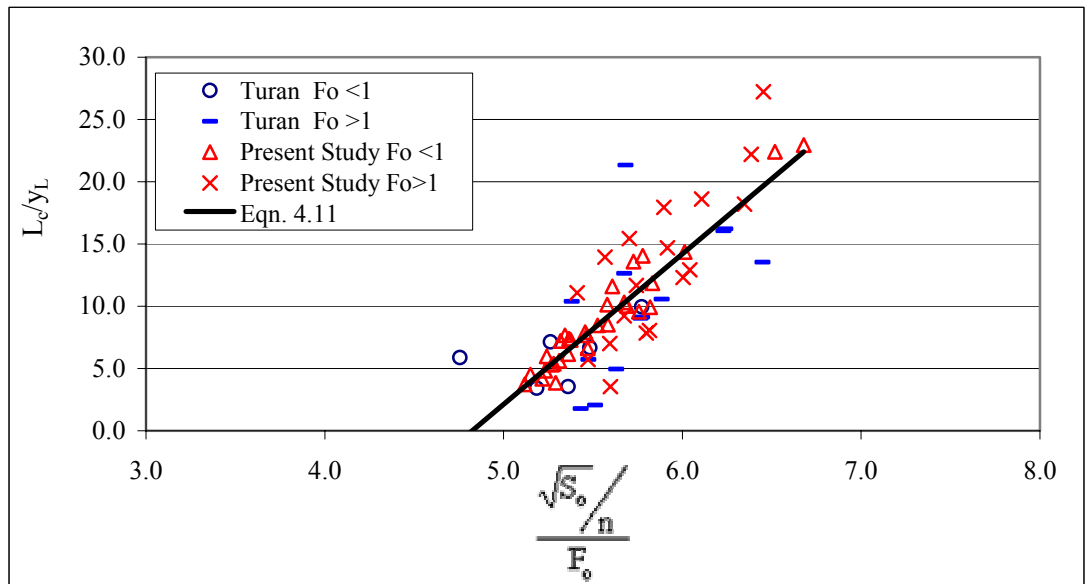
Figure 4.10 Variation of L_c/y_L with $\dfrac{\sqrt{S_o}/n}{F_o}$ in both flow conditions

Table 4.3 Equations and the R^2 values for relationship between L_c/y_L and $\dfrac{\sqrt{S_o}/n}{F_o}$

Equation Number	Flow Condition	Equation	R^2
4.9	Sub	$\dfrac{L_c}{y_L} = 11.5\left(\dfrac{\sqrt{S_o}/n}{F_o}\right) - 54.9$	0.86
4.10	Super	$\dfrac{L_c}{y_L} = 13.8\left(\dfrac{\sqrt{S_o}/n}{F_o}\right) - 68.3$	0.53
4.11	Sub and Super	$\dfrac{L_c}{y_L} = 12.1\left(\dfrac{\sqrt{S_o}/n}{F_o}\right) - 58.3$	0.68

4.10 Variation of $\dfrac{y}{y_L} * \dfrac{F_o}{\sqrt{S_o}/n}$ with x/L$_c$ in Subcritical and Supercritical Flow

Typical schematic diagram of critical depth distance from the brink, L_c (i.e. $L_{c,sub}$) and corresponding critical depth, y_L (i.e. y_c) are given in Figure 4.7 for subcritical flow condition. According to x and y coordinate system, water surface profile has been obtained (see Figure 4.7). In order to obtain a dimensionless form, x and y coordinate points of water surface are divided by the critical depth y_L (i.e. y_c) and the distance of critical depth from the brink L_c, respectively in Figure 4.11. An appreciate curve is fitted for these points, equation and respective RMS values are given Table 4.4.
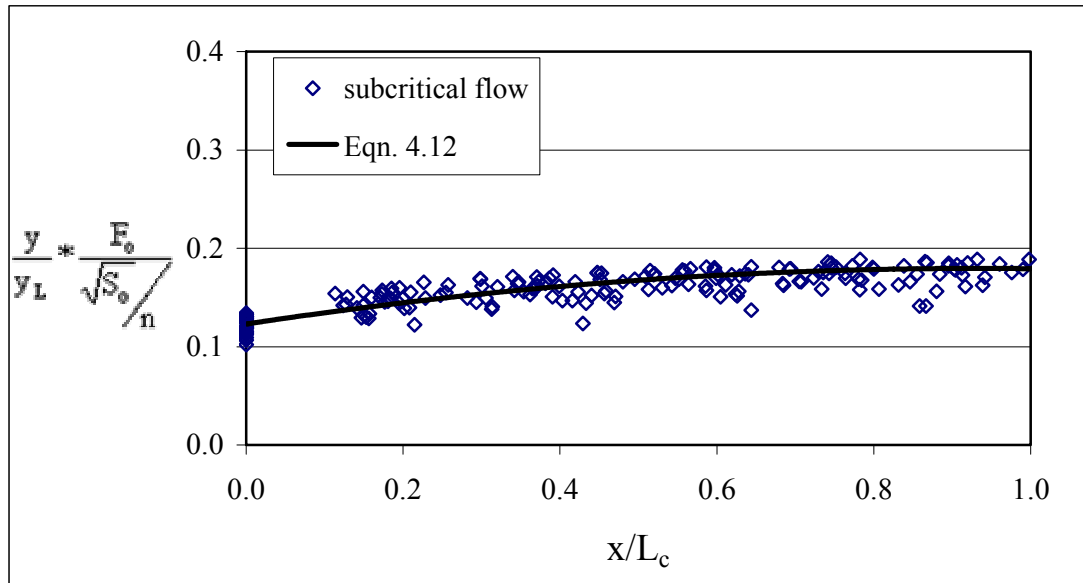
Figure 4.11 Variation of $\dfrac{y}{y_L} * \dfrac{F_o}{\sqrt{S_o}\Big/n}$ with x/L_c

For supercritical flows condition, according to x and y coordinate system water surface profile has been obtained in Figure 4.12. In order to obtain a dimensionless form, x and y coordinate points of water surface are divided by normal depth y_L (i.e. y_o) and the distance of critical depth from the brink L_c (i.e. $L_{c,super}$), respectively. An appreciate curve is fitted for these points, equation and respective RMS values are given Table 4.4.
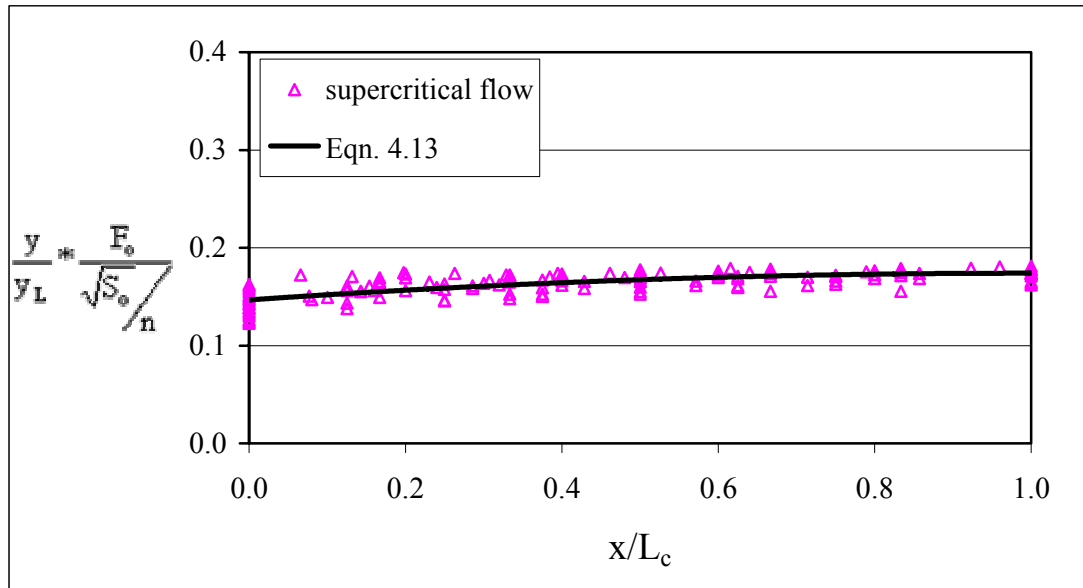
Figure 4.12 Variation of $\dfrac{y}{y_L} * \dfrac{F_o}{\sqrt{S_o}/n}$ with x/L$_c$

Combination of both conditions is given on the same graph to see the similarity between subcritical and supercritical flow. This situation is depicted in Figure 4.13. For both cases a curve fitted. Equation and RMS values are given in Table 4.4.
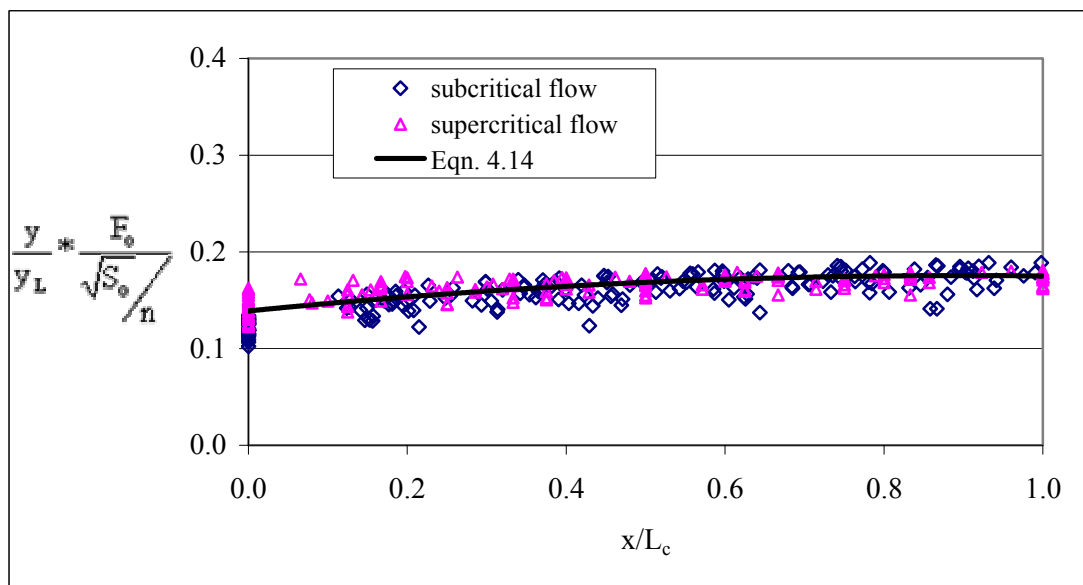
Figure 4.13 Variation of $\dfrac{y}{y_L} * \dfrac{F_o}{\sqrt{S_o}/n}$ with x/L$_c$ for both conditions

Table 4.4 Water surface profiles according to x and y coordinate system

Equation Number	Flow Condition	Equation	RMS
4.12	Sub	$\dfrac{y}{y_L} * \dfrac{F_o}{\sqrt{S_o}/n} = -0.065\left(\dfrac{x}{L_c}\right)^2 + 0.122\left(\dfrac{x}{L_c}\right) + 0.123$	0.011
4.13	Super	$\dfrac{y}{y_L} * \dfrac{F_o}{\sqrt{S_o}/n} = -0.028\left(\dfrac{x}{L_c}\right)^2 + 0.055\left(\dfrac{x}{L_c}\right) + 0.147$	0.009
4.14	Sub and Super	$\dfrac{y}{y_L} * \dfrac{F_o}{\sqrt{S_o}/n} = -0.046\left(\dfrac{x}{L_c}\right)^2 + 0.082\left(\dfrac{x}{L_c}\right) + 0.14$	0.019

4.11 Flow Chart to Design a Free Overfall

The results which are presented in the previous sections can be used by engineers to design a free overfall by following charts given below;

1) Estimate of S_o, n.

2) Measurements of the brink depth, y_e in the field.

3) By using of S_o, n and y_e, calculate the discharge, q.

4) Determine the Froude Number, F_o.

5) Calculate the L_c by using of Equation 4.11.

6) Calculate the water surface profile along the L_c by using of Equation 4.14.

CHAPTER 5

CONCLUSIONS

In the present study the effects of the roughness, the slope, the Froude number and normal depth on the rectangular free overfall at large and on the brink depth in particular are investigated by combining other researchers' studies. An empirical relationship is obtained to confirm previous studies in predicting discharge. Thus the channel discharges are predicted and are compared with measured values. Also $L_{c,sub}$, critical depth distance from the brink in subcritical flow condition and $L_{c,super}$, distance the flow begins to be affected from the brink in supercritical flow condition are related with flow conditions. By this experimental study the following have been discerned:

1) There is a constant ratio between y_e and y_c (the brink depth and theoretical critical depth) for whole slopes in subcritical flow regime and for the slopes stating supercritical flow condition, y_e/y_c values show a decreasing trend in with increasing slope.

2) As y_e/y_c ratio decreases with the increase of F_o number.

3) As y_e/y_c values decreases with $\dfrac{S_o}{S_c}$ ratio increases.

4) The brink depth ratio seems to be independent of upstream Froude number for supercritical flows, while it decreases with increasing upstream Froude number. In other words, the relation between y_e/y_c and y_o/y_c shows different characteristics in subcritical and supercritical flows. It is constant for subcritical flow and polynomial for supercritical flow.

35

5) Based on the findings of this study, two equations of the form for discharge prediction Tiğrek et al. (2005) is confirmed;

$$q = 5.55 y_e^{3/2} \qquad \text{for} \qquad \frac{\sqrt{S_o}}{n} \le 5$$

$$q = \left(\frac{n}{0.361n - 0.084\sqrt{S_o}}\right)^{3/2} y_e^{3/2} \qquad \text{for} \qquad \frac{\sqrt{S_o}}{n} > 5$$

6) Relationships are obtained between $\dfrac{y}{y_L} * \dfrac{F_o}{\sqrt{S_o}/n}$ with x/L_c. These relations are proposed in one equation for both subcritical and supercritical flow conditions;

$$\frac{y}{y_L} * \frac{F_o}{\sqrt{S_o}/n} = -0.046\left(\frac{x}{L_c}\right)^2 + 0.082\left(\frac{x}{L_c}\right) + 0.14$$

7) Relationships are obtained between L_c/y_L with $\dfrac{\sqrt{S_o}/n}{F_o}$. This relations are proposed in one equation for both subcritical and supercritical flow conditions;

$$\frac{L_c}{y_L} = 12.1\left(\frac{\sqrt{S_o}/n}{F_o}\right) - 58.3$$

Have been obtained for the determination of discharge in a rectangular and/or wide channel. The validity of the above equation has been secured by the use of findings of independently obtained data of the previous works.

In this form, with the known characteristics S_o and n, for the determination of discharge q, the measurement of the brink depth y_e is sufficient.

36

REFERENCES

Ahmad, Z. (2003), "Quasi-Theoretical end-depth-discharge relationship for rectangular channels*", J. Irrig. and Drain. Eng., ASCE*, 129(2), 138-141.

Bauer, S.W. and Graff, W.H. (1971), "Free overfall as flow measuring device", *J. Irrigation and Drainage Div.*, *ASCE*, Vol. 97, No. 1.

Chow, V.T. (1959), "Open-Channel Hydraulics", *The McGraw-Hill Book Company*, Tokyo, 206.

Davis, C.A., Ellet, B.G.S. and Jacob, R.P. (1998), "Flow measurements in sloping channels with a rectangular free overfall", *J. Hydraulic Engrg.*, *ASCE*, Vol. 124, No. 7.

Ferro, V. (1992), "Flow measurement with rectangular free overfall", *J. Irrigation and Drainage Engrn.*, *ASCE*, Vol. 118, No. 6.

Fırat, C.E. (2004), "Effect of roughness on flow measurements in sloping rectangular channels with free overfall, *M.Sc. Thesis, METU*, Ankara.

Gupta, R.D., Jamil, M. and Mohsin, M. (1993), "Discharge prediction in smooth trapezoidal free overfall-(positive, zero and negative slopes)", *J. Irrigation and Drainage Div.*, *ASCE*, Vol. 119, No. 2.

Guo, Y. (2005), "Numerical Modeling of Free Overfall", *J. Irrigation and Drainage Eng., ASCE*, 131(2), 134-138.

Gürsoy, E. (2002), "water jet pumps with multiple nozzles", *M.Sc. Thesis, METU*, Ankara.

Hager, W. (1983), "Hydraulics of plane free overfall", J. *Hydraulic Engng., ASCE,* Vol. 109, No. 12.

Kraijenhoff, D.A. and Dommerholt, A.(1977), "Brink depth method in rectangular channel", *J. Irrigation and Drainage Div.*, *ASCE*, 103(2).

Marchi, E. (1993), "On the free overfall", *J. Hydraulic Res.*, Delft, The Netherlands, 31(6).

Montes, J. S. (1992), "A potential flow solution for the free overfall", *Water, Maritime and Energy, ICE*, London, 96.

Özsaraç, D. (2001), "Potential flow solution for the free overfall", *M.Sc. Thesis, METU*, Ankara.

Rajaratnam, N. and Muralidhar, D. (1964a), "End depth for circular channels", *J. Irrigation and Drainage Div.*, *ASCE*, Vol. 90, No. 2.

Rajaratnam, N. and Muralidhar, D. (1968), "Characteristics of the rectangular free overfall", *J. Hydraulic Research*, Vol. 6 No. 3.

Rajaratnam, N. And Muralidhar, D. and Belatos, S. (1976), "Roughness effects on rectangular free overfall", *J. Hydraulic Div. ASCE*, Vol. 102 No. 5.

Rouse, H. (1936), "Discharge characteristics of the free overfall", *Civil Engineering*, *ASCE,* Vol. 6, No. 4.

Southwell, R. and Vaisey, G. (1946), "Relaxation methods applied to engineering problems, fluid motions characterised by 'free' streamlines", *Philosophical Trans. Royal Soc.*, London, Ser a, 240.

Strelkoff, T. and Moayeri, M. S. (1970), "Pattern of potential flow in a free overfall", *J. Hydr. Div.*, *ASCE,* 96(4).

Tiğrek, Ş., Fırat, C. E. and Ger, A.M. (2005), "Effect of roughness on flow measurements in sloping rectangular channels with free overfall", unpublished paper.

Turan, Ç.K. (2002), "Flow measurements in sloping rectangular channels with free overfall", *METU*, Ankara.
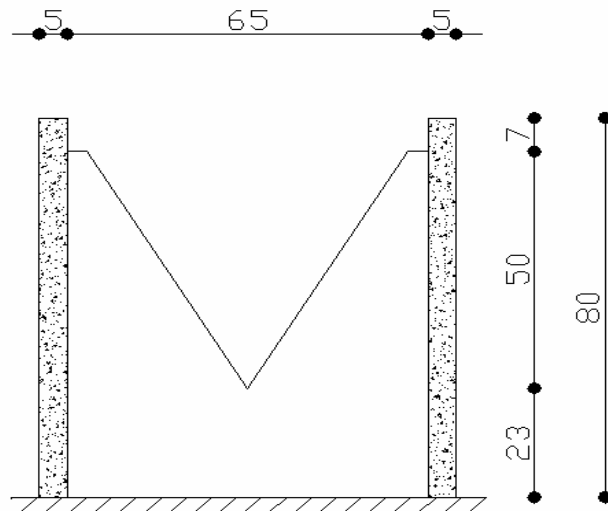
APPENDIX A

TRIANGULAR WEIR and CALIBRATION CURVE
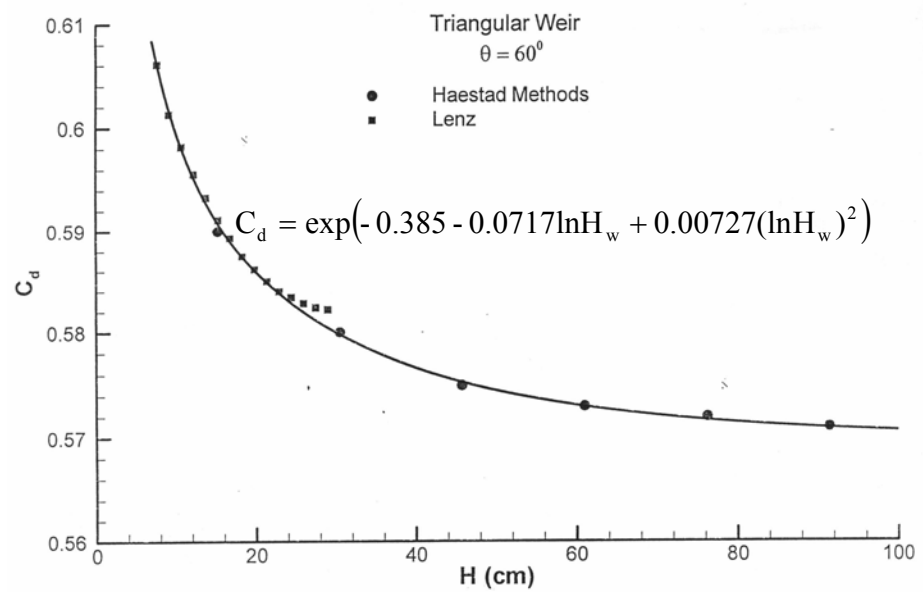

Figure A.1 The triangular weir section

$$C_d = \exp\left(-\,0.385 - 0.0717 \ln H_w + 0.00727(\ln H_w)^2\right)$$

Figure A.2 Calibration curve of triangular weir (After Gürsoy, 2002)

APPENDIX B

EXPERIMENT CONDUCTED IN THE PRESENT STUDY and MANNING'S

ROUGHNESS COEFFICIENT

Table B.1 The data for the channel

Number of Set	S_o	n	S_c	Q (lt/s)	y_e (cm)	y_o (cm)	y_c (cm)	L_c (cm)	F_o
1	0.00063	0.0147	0.00836	8.14	1.27	4.19	1.89	21.9	0.3
	0.00063	0.0147	0.00719	18.88	2.24	7.08	3.31	23.85	0.32
	0.00063	0.0147	0.00637	42.3	3.82	11.87	5.67	25.56	0.33
	0.00063	0.0147	0.00609	61.36	5.03	15.15	7.27	26.98	0.33
2	0.00166	0.0147	0.00822	8.88	1.4	3.27	2	28.13	0.48
	0.00166	0.0147	0.00805	9.98	1.41	3.51	2.17	29.45	0.48
	0.00166	0.0147	0.00674	28.21	2.89	6.7	4.33	33.25	0.52
	0.00166	0.0147	0.00638	41.57	3.84	8.57	5.61	33.51	0.53
3	0.00188	0.0147	0.01141	1.75	0.46	1.17	0.68	15.54	0.44
	0.00188	0.0147	0.00710	20.46	2.29	5.27	3.49	27.65	0.54
	0.00188	0.0147	0.00658	33.42	3.27	7.18	4.85	27.19	0.55
	0.00188	0.0147	0.00630	45.81	3.91	8.77	5.98	28.89	0.56
4	0.00194	0.0147	0.00775	12.28	1.68	3.81	2.49	25.62	0.53
	0.00194	0.0147	0.00705	21.2	2.46	5.34	3.58	27.41	0.55
	0.00194	0.0147	0.00644	38.9	3.7	7.82	5.36	28.81	0.57
	0.00194	0.0147	0.00622	51	4.44	9.3	6.42	26.83	0.57
5	0.003	0.0147	0.00773	12.48	1.67	3.36	2.51	24.05	0.65
	0.003	0.0147	0.00718	18.97	2.21	4.35	3.32	28.27	0.67
	0.003	0.0147	0.00652	35.73	3.5	6.46	5.07	31.24	0.69
	0.003	0.0147	0.00624	49.68	4.41	7.96	6.31	33.5	0.71
6	0.00388	0.0147	0.00774	12.4	1.66	3.09	2.5	24.8	0.73
	0.00388	0.0147	0.00671	29.16	3.06	5.25	4.43	29.24	0.77
	0.00388	0.0147	0.00644	38.66	3.62	6.26	5.34	38.83	0.79
	0.00388	0.0147	0.00620	52	4.43	7.55	6.51	25.05	0.8
7	0.00506	0.0147	0.00973	3.76	0.79	1.38	1.13	25.3	0.74
	0.00506	0.0147	0.00759	13.81	1.76	3.04	2.69	31.86	0.83
	0.00506	0.0147	0.00687	24.92	2.64	4.38	3.99	40.39	0.87
	0.00506	0.0147	0.00630	45.78	4.17	6.4	5.98	44.15	0.9

Table B.1 (Cont'd)

Number of Set	S_o	n	S_c	Q (lt/s)	y_e (cm)	y_o (cm)	y_c (cm)	L_c (cm)	F_o
8	0.00613	0.0147	0.00799	10.41	1.47	2.42	2.23	31.96	0.89
	0.00613	0.0147	0.00707	20.86	2.33	3.7	3.54	35.46	0.94
	0.00613	0.0147	0.00664	31.43	3.09	4.77	4.65	39.31	0.96
	0.00613	0.0147	0.00626	48.24	4.21	6.23	6.19	-	0.99
9	0.00728	0.0147	0.00827	8.61	1.36	2.04	1.96	25.97	0.94
	0.00728	0.0147	0.01530	21.13	2.4	3.54	3.57	-	1.01
	0.00728	0.0147	0.01530	31	3.15	4.48	4.61	62.5	1.04
	0.00728	0.0147	0.01530	47.82	4.22	5.87	6.15	65	1.07
10	0.01325	0.0147	0.00771	12.65	1.61	2.15	2.54	40	1.28
	0.01325	0.0147	0.00716	19.32	2.14	2.78	3.36	50	1.33
	0.01325	0.0147	0.00662	31.89	2.98	3.79	4.7	35	1.38
	0.01325	0.0147	0.00618	53.84	4.25	5.25	6.66	30	1.43
11	0.019775	0.0147	0.00834	8.26	1.18	1.47	1.91	40	1.48
	0.019775	0.0147	0.00697	22.74	2.23	2.72	3.75	40	1.62
	0.019775	0.0147	0.00658	33.17	2.83	3.43	4.82	40	1.67
	0.019775	0.0147	0.00627	47.41	3.59	4.28	6.12	30	1.71
12	0.028375	0.0147	0.00789	11.12	1.36	1.58	2.33	35	1.79
	0.028375	0.0147	0.00697	22.75	2.14	2.44	3.75	30	1.91
	0.028375	0.0147	0.00653	35.17	2.8	3.18	5.01	25	1.98
	0.028375	0.0147	0.00615	56.12	3.81	4.25	6.85	15	2.05
13	0.038688	0.0147	0.00757	13.95	1.49	1.65	2.71	30	2.11
	0.038688	0.0147	0.00689	24.56	2.18	2.32	3.95	30	2.21
	0.038688	0.0147	0.00643	39.38	2.85	3.1	5.41	25	2.3
	0.038688	0.0147	0.00622	50.81	3.36	3.63	6.41	56	2.35

Table B.2 Experiment conducted on adverse slopes

| Number of Set	S_o	n	S_c	Q (lt/s)	y_e (cm)	y_c (cm)	y_e/y_c
14	-0.00163	0.0147	0.00779	11.9	1.86	2.44	0.76
	-0.00163	0.0147	0.00677	27.41	2.94	4.25	0.69
	-0.00163	0.0147	0.00631	45.44	4.17	5.95	0.70
15	-0.00669	0.0147	0.00696	23.02	2.57	3.78	0.68
	-0.00669	0.0147	0.00637	42.3	4.04	5.67	0.71
16	-0.01288	0.0147	0.00712	20.05	2.54	3.45	0.74
	-0.01288	0.0147	0.00640	40.89	4.2	5.54	0.76
17	-0.02088	0.0147	0.00754	14.3	2.2	2.75	0.80
	-0.02088	0.0147	0.00681	26.4	3.12	4.14	0.75
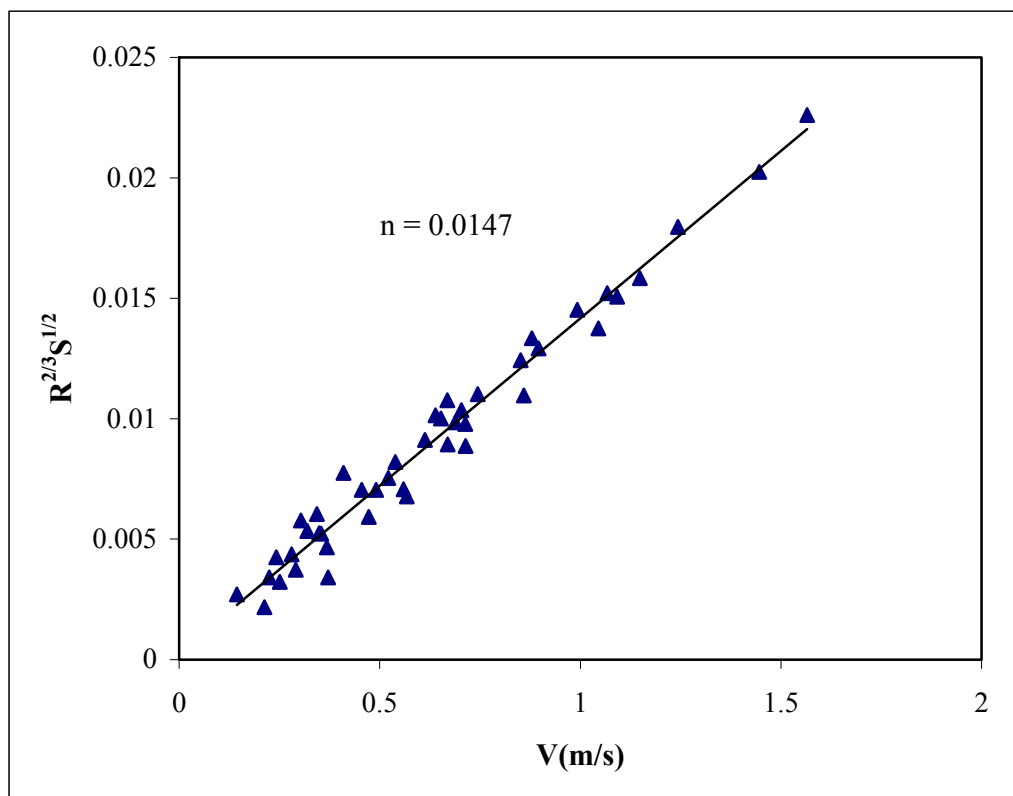
Figure B.1 Manning's roughness coefficient for the channel (After Fırat, 2004)